An Approach to On-line Welding Control through an Artificial Vision System

Lanzetta M., Tantussi G., and Santochi M.
Dipartimento di Ingegneria Meccanica, Nucleare e della Produzione
Università degli studi di Pisa, via Bonanno Pisano, 25/B – 56126 Pisa

Summary

This study deals with the development and test of vision algorithms to be integrated in a robotised welding system. Two views have been considered: the molten weld pool and the arc; the joint profile obtained by projecting a laser light few millimetres behind.
An experimental facility has been set-up in order to simulate all possible defects for both the off-line analysis in the algorithm implementation phase and for the on-line tests.
A wide variety of defects have been produced and images have been collected in a database. The algorithm for the image analysis is based on the extraction of geometric features from the binarised images of the hot pool and of the cold joint. The main problems of pre-processing and feature extraction are addressed. The main experimental results for the system performance assessment and the detectable defects are provided.

Key words: Welding, On-line Control, Image Analysis

1. Introduction

The global competitiveness and the personnel protection and safety involve an increase of the process automation even in industries specialised in welding with lot or prototypical production. The adoption of a welding robot requires the use of sensors for the on-line process monitoring and control. The sensor task is modifying the process parameters to overcome unforeseen events like geometrical bevel changes or to detect the presence of dirt or the lack of the protecting gas.
Considering that, according to the industrial needs, the sensor task is to simulate the operator's action, the image analysis and processing is mainly based on the firm experience tested and validated on the field for many years. However this often represents an implicit knowledge based on sensations and practical hints.
It should be pointed-out that with respect to standard vision applications, welding images are characterised by the high rapidity and intensity of changes and by the

presence of many disturbing elements.
The main problem of the on-line image acquisition is the high arc emission intensity. The spectrum analysis can be found in [1] and [2]. In all available applications filters are used. In addition, the arc emission problem is approached by acquisitions when the tension reaches a minimum, like in [3] and [4], or zero by pulsed tension and current [5].
All applications belong to two categories: pool or joint observation. The root penetration is considered the most important and investigated problem; it could be assessed with a bottom view, but this method has accessibility problems in most application. For this reason, several alternatives have been proposed: in [6] and [7] a correlation respectively between the pool dimension and the 3-D shape of the pool and the welding parameters is described; in [8] the weld pool oscillation is considered. In [9] and [10] the joint features are considered instead. In [11]a neural method is described to detect undercut and overlap.
Profile extraction methods are available in the literature from many applications with structured light [12]. In welding, structured light is also used for seam tracking and many applications are already available. In both cases the arc emission must be filtered and previous experience can be used. In [4] the system calibration and the acquisition error correction are described. The main difference is the sensor position with respect to the torch. In [6] e [7] a high power pulsed laser is used, in order to increase the signal to noise ratio; in these cases, structured light is used for the pool analysis. In [6] a grid is used instead of a line.
From the analysis of literature, several systems have been proposed, but it seems that a method to characterise and recognise the most important defects is not yet available.
This study is part of a research program whose final target is to develop a vision sensor to be integrated in a completely automatic robotised welding system. The hardware development is described in [13]; the image analysis aspects are described here. However for the implementation and test of the necessary algorithms an experimental facility has been developed and weld tests have been performed in different conditions.

2. System configuration

From the analysis of the literature, to obtain the necessary information on the process, two views and cameras are sufficient and have been adopted: a view of the pool and a view of the joint, by projecting a laser stripe. A system configuration scheme is shown in Figure 1. The main elements that can be retrieved from the two images are also indicated. Images are obtained both in interlaced and non-interlaced mode at CCIR resolution. Considering the relative movement between the sensor and the parts, a laser stripe is sufficient for 3-D reconstruction, instead of a grid. The observed joint, addressed to as the “cold” joint, is still at a high temperature, but its aspect will remain unchanged for the whole weld life, apart from cold cracks that may occur at any time. So this analysis is a sort of on-line visual inspection.

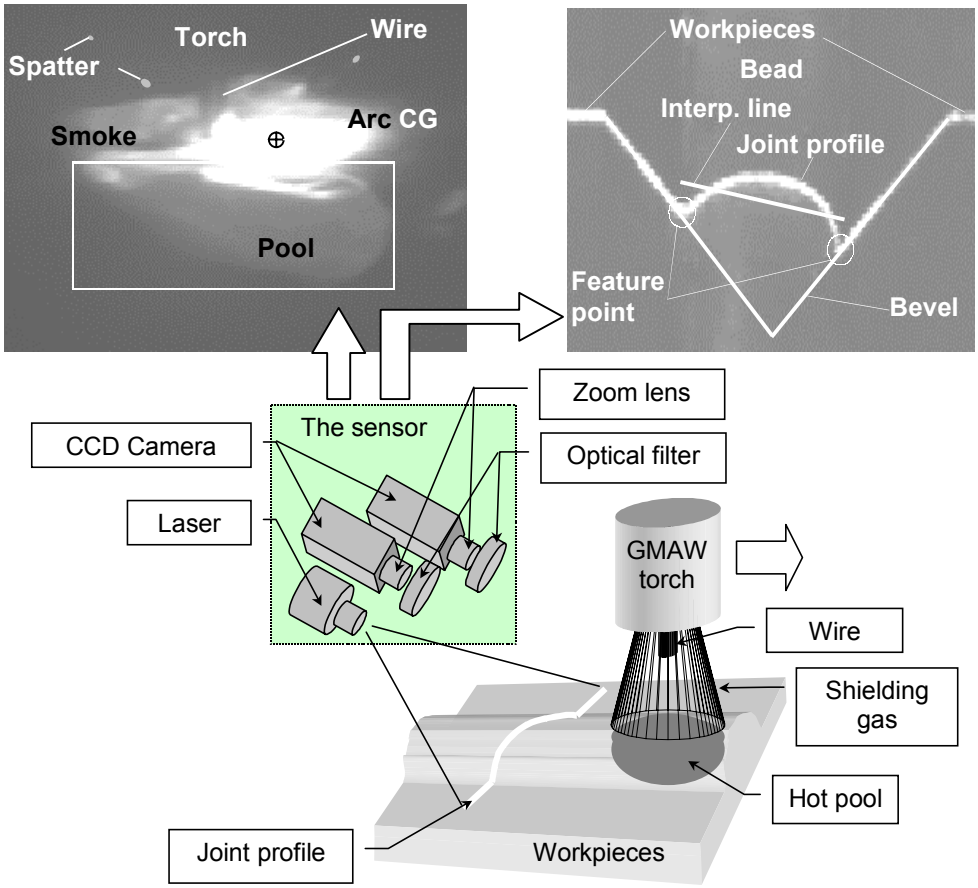

Figure 1: “Hot” and “cold” view (top). The system configuration during tests and for the final version (bottom).

3. Experimental

The main task of the developed facility is the acquisition of images of good and defective joints to develop and test the algorithms. A GMAW torch has been installed on a fixed support with a sliding table holding the parts. Butt joint with a 90° bevel angle have been performed, in *short arc* for the root pass and *spray arc* for the intermediate and final passes. Two cameras external to the working area are used. A 10% optical neutral density filter has been selected in order to reduce the saturation problem in the pool acquisition.

3.1 *Methods to artificially create defects and defect morphology*
The following defects have been created with the methods indicated, coming from

the industrial experience of the partners involved in the project. Most information can be obtained from the joint observation. Additional information on the process can be obtained from the pool analysis.
Surface *porosity* can be obtained in two ways: by putting some grease in the bevel to produce gas bubbles or by discontinuing the protection gas to allow fast oxidation. Their appearance is a pool boil and one or several small holes on the joint surface.
The *lack of fusion* (Figure 1 top right) can be obtained by reducing the heat input, hence by reducing tension, as the current reduction is usually bound to the wire feed speed. On the opposite, by increasing the heat input, an *undercut* can be obtained. They are characterised by a groove on the two sides of the cold joint. The *excess* or *lack of deposited metal* can be obtained in three different situations: in the root, in an intermediate or in the final pass and is characterised by different effects such as *partial* or *incomplete penetration* and *overlap*. From a morphological point of view the following distinction only is sufficient: the fillet between bead and bevel should be smooth. In addition, the joint profile should be concave in all cases except for the final pass, where it must be convex. These defects and the lack of fusion can be observed from the cold joint and are characterised by the sign and value of the profile concavity/convexity.
Spatters (Figure 1 top left) have the following problems: they can be inclusions for successive passes, they denote that parameters were not optimal, and they are possible corrosion attack zones. They can be easily obtained at high current values.
Hot cracks only could be observed by the sensor during welding.

4. Image analysis algorithms and experimental tests

The analysis of images is based on two steps: preprocessing and feature extraction.

4.1 *Preprocessing*

Concerning the pool analysis, the main problem is the separation between the pool and the arc.
The light distribution of the arc emission is approximately decreasing as a function of the distance from that line. The consequence is that changing the binarisation threshold, a different arc size is obtained. For this reason, during acquisition the dimension of the saturated area, which includes pixels at the maximum available light intensity, is kept below the pool width, as shown in Figure 1 (top left). The effect of reducing the light input is to decrease the saturated area corresponding to the arc within the image by concentric circles. However the big difference between the arc and the pool emission does not allow to completely remove the saturated area belonging to the arc without making the pool disappear. On the opposite, the pool intensity is approximately constant as it depends on the metal temperature. The pool extraction is then based on binarisation at a threshold determined for each image by eliminating the background area.
The points belonging to the background (bg) satisfy the following expression:

$$I_{bg} < I_m(x, y) + 3 \times I_\sigma(x, y) : x, y \in bg$$

where intensities I_m and I_σ are respectively the mode and the standard deviation of the grey level distribution and have the typical values of 8 and 2. The mode is used instead of the mean grey level because it is not affected by the presence of noise and of spatters.
To obtain information on the arc, the saturated area only is considered with a binarisation at higher threshold (200). The different areas are shown in Figure 1

Table I: Features tested for each defect and corresponding error.

Defect and process information	Source	Description: feature	Error (Filtered) [± % of avg. value] Notes
Porosity	Cold	Profile interruption	Detectable. Ambiguity with spatters
Penetration	Hot	Pool dimensions: area – perimeter – width – height	9 (8.6) – 15 (11) – 10.3 – 10.7
	Cold	Profile concavity: signed addition of distances between profile and interpolation straight line	(2.4)
Underfill, overlap, lack of fusion	Cold	See above	
Asymmetry	Cold	Inclination of the interpolation straight line (Figure 1 top right)	12.5
Deposition	Hot	Pool dimension: area, width	9 (8.6) – 10.3
	Cold	Joint width: distance between feature points	(2.1)
		Deposited metal section and profile concavity	(1.7)
Arc instability	Hot	Arc dimension (blow-out): area	20 (12)
	Hot	Arc lateral displacement: hor. co-ordinate of the saturated area centre of gravity (CG) (Figure 1 top right)	Detectable
Smoke	Hot	Pool and arc dimension	Detectable
Spatters	Hot	Blob number	Detectable
	Cold	Profile interruption	Detectable. Ambiguity with porosity
Actual tension	Hot	Wire length: vert. co-ordinate of the saturated area CG	9 (6)

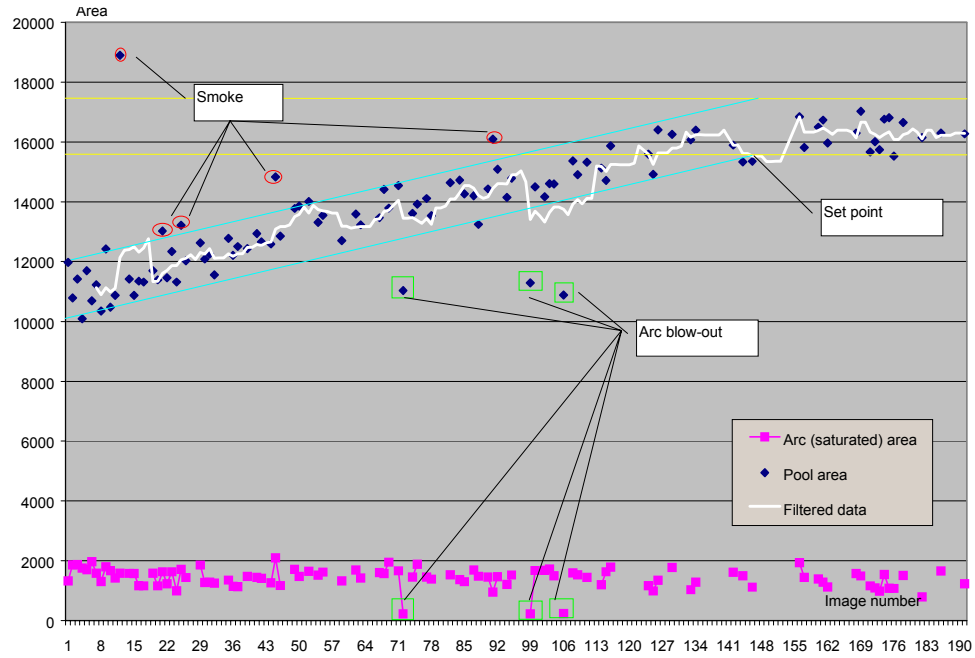

Figure 2: Example of feature extracted from a sequence of images of the molten weld pool.

(top left) and are used for feature extraction.
For the profile extraction, a fixed threshold binarisation is again used. The value is determined at system set-up by trials and depends on the external and laser light intensities.

4.2 *Feature extraction*
The analysis of the hot pool is mainly based on a blob analysis on the regions determined with pre-processing. The profile analysis is based on the extraction of geometric features to characterise the different profiles that can be obtained if a defect is present. The main features tested, their significance and definition are summarised in Table I. The main results of the tested algorithms are also reported in the table.
The following defects have not been considered in the analysis: *undercut* and *slag*. *Cracks* are not visible with the available sensor resolution. The *transfer mode*, *short* or *spray arc*, cannot be deduced from images only because of the phenomenon rapidity. The available resolution does not allow a microscopic arc observation. The macroscopic feature variations are not univocal and may be confused with parameter changes.
From the sequence of images (Figures 2 and 3), the following information can be obtained.
1. The feature error is calculated as the envelope of displayed values. This error

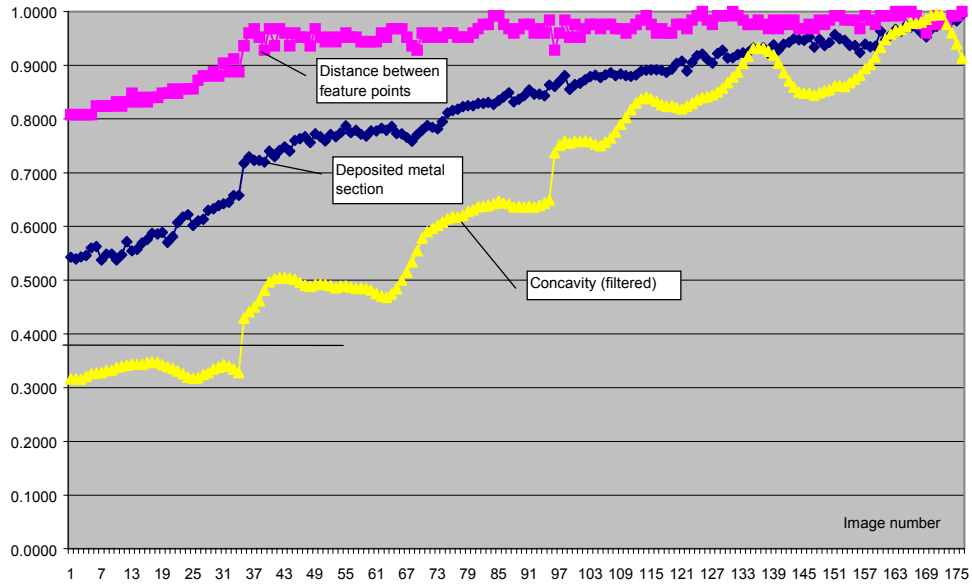

Figure 3: Example of comparison and correlation between features (normalised) extracted from a sequence of images of the joint profile.

is mainly due to the phenomenon variability. The effect of changing the acquisition rate has also been tested. The error due to the presence of noise has been manually removed and still requires the implementation of automatic procedures for the on-line analysis.

2. By filtering data (a triangular filtered profile on 7 points is displayed) the error can be reduced, but a delay in the control is obtained.

4.3 *Examples of defect monitoring*

In the image sequence displayed in Figure 2, the current is increased up to the correct value which is kept constant starting from image 150. The presence of *smoke* (Figure 1 top left) is shown by the pool area peaks. On the opposite, the lower peaks show the *arc blow-out*, that can be verified with the lower peaks of the saturated area, which remains constant for the whole sequence.

The lower half pool only is considered, as the front part is obstructed by the torch. The other pool features that can be correlated with *penetration* have a similar trend, with the errors displayed in Table I. Width and height are the dimensions of the box circumscribed around the pool (Figure 1 top left).

In Figure 3, the current is again increased and an *overlap* is obtained starting from image 40. A possible threshold for this defect is displayed. In the first part, concavity remains constant. In this condition, the joint width, calculated as the distance between the feature points, and the deposited metal section have the same trend, but the second has a higher accuracy as it is less sensible to local

errors. The correlation between the other two features, which have the same trend, is shown in the second part of the sequence, where the joint width remains approximately constant. The feature errors are indicated in Table I.

5. The control strategy

The described system can be exploited at three levels: (i) support to the operator with additional information on the process or for product certification, (ii) defect detection, (iii) process control. The final target is (iii) but some extra information on the process can also be obtained for task (i).
Industrial or international standards state the acceptability of a defect. Porosity, cracks and lack of fusion are the most critical and it is necessary to re-make the weld. The other defects are tolerated below a predefined length, so it is sufficient to correct the parameters in case they are detected.
Porosity can be confused with the presence of spatters on the profile, but considering that it s a very critical defect, a warning message is provided if any profile interruption is detected. Concerning the other defects, all features are extracted in parallel and a separate action is performed. At present no conflicts have been recorded, but a synergy of some of them, as indicated in Table I, e.g. for the deposition.
The selection of features is based on their sensitivity and correlation with defects which has been assessed on the available images, e.g. the pool area versus perimeter, width and height from Table I and so on. Considering the strong features dependence on the different welding conditions that may affect their performance, all of them should be included in the control for redundancy purposes.

6. Conclusions

The described system represents a first attempt to develop the necessary algorithms for a sensor able to recognise all visible defects.
In this study, twenty defect types and information on the process have been dealt with. All of them have been created artificially and analysed, except the undercut and the slag presence. For each, several features have been tested and compared to estimate their correlation and error. The more reliable and accurate have been described. The errors obtained in defect detection have been acceptable if compared with the required accuracy of industrial welding.
Ongoing activity concerns the test of the control strategy through the on-line system integration, and experiments on an industrial case. The following tasks are still necessary: (i) software optimisation to allow the required frame rate in the cold analysis; (ii) reduction of noise on features by filtering and by improving the algorithm performance according to present analysis; (iii) a direct correlation of images to the instantaneous welding parameters.

Acknowledgements

This study has been developed within the national MURST project “Sistemi di

Produzione Innovativi" Tema 5 – Sistema automatizzato flessibile e adattativo di saldatura, Linea 2.3 – Controllo di processo: controllo on-line.

References

[1] Kim, E.W., Allemand, C. and Eagar, T.W.; Visible light emission during gas tungsten arc welding and its application to weld image improvement, Welding Research Supplement, Dec. 1987: 369-377

[2] Li, Y. and Middle, J.E.; Machine vision analysis of welding region and its application to seam tracking in arc welding, Journal of Engineering Manufacture, Proc. Instn. Mech. Engrs., 1993, 207: 275-283

[3] Wu, C.S. and Liu, Y.C.; Rule-based control of weld bead width in pulsed gas tungsten arc welding (GTAW), Journal of Engineering Manufacture, Proc. Instn. Mech. Engrs., 1996, 210: 93-98

[4] Wu, C.S.; Vision-based determination of welding groove geometry in MAG welding process, International Journal for the Joining of Materials, 1994, 6: 152-156

[5] Stone, D.A., Smith, J.S. and Lucas, J.; Sensor for automated frontface weldbead area control, Measurement, Science and Technology, IEE Proc., 1994, 5: 93-99

[6] Kovacevic, R. and Zhang, Y.M.; Real-time image processing for monitoring of free weld pool surface, Journal of Manufacturing Science and Engineering, Transactions of the ASME, May 1997, 119: 161-169

[7] Kovacevic, R. and Zhang, Y.M.; Role of welding parameters in determining the geometrical appearance of weld pool, Journal of Engineering Materials and Technology, Transactions of the ASME, October 1996, 118: 589-596

[8] den Ouden, G., Xiao, Y.H. and Hermans, M.J.M.; The role of weld pool oscillation in arc welding, International Journal for the Joining of Materials, 1994, 5: 123-129

[9] Zhang, Y.M. and Kovacevic, R.; Real-time sensing of sag geometry during GTA welding, Journal of Manufacturing Science and Engineering, Transactions of the ASME, May 1997, 119: 151-160

[10] Zhang, Y.M., Kovacevic, R. and Wu, L.; Closed-loop control of weld penetration using front-face vision sensing, Journal of System and Control Engineering, Proc. Instn. Mech. Engrs., 1993, 207: 27-34

[11] Inoue, K. and Yi, N.; Application of a neural network to visual inspections of weld beads, Welding International, November 1993: 857-862

[12] Rioux, P.; 1986, Laser range-finder based on synchronised scanners, in Pugh, A. (ed.), Robot sensors, Vol. 1 – Vision, Springer-Verlag: 175-190.

[13] Mariotti, F. and Pecoraro, L.; 1999, MWS – Multiple Weld Sensor, Proc. of IV Aitem Conf., Brescia (Italy), 13-15 Sept. 1999